Pergamon

Int. J. Solids Structures Vol. 33, No. 20–22, pp. 3035–3056, 1996

0020–7683/96 $15.00 + .00

0020–7683(95)00264–2

STOCHASTIC STRUCTURAL INTERFACE DEFECTS IN FIBER COMPOSITES

MARCIN KAMIŃSKI
Division of Mechanics of Materials, Technical University of Lodz, Poland

and

MICHAŁ KLEIBER
Institute of Fundamental Technological Research, Polish Academy of Sciences, Warsaw, Poland

Abstract—In this paper the new idea of homogenization of stochastic interface structural defects in the matrix of a fiber composite, recently proposed by the first author, is extended to the contact zones of both components. The physical mechanism of the occurrence of interface defects is described and different versions of location of these defects on fiber–matrix boundary are tested using the stochastic finite element method (SFEM). Two first moments of the displacement random fields are computed and a new SFEM formulation for such problems is proposed. Copyright © 1996 Elsevier Science Ltd.

1. INTRODUCTION

Most of the current theories which characterize mechanical properties of fiber composite materials assume that the fibers form some kind of regular array (square, hexagonal, etc.). Unfortunately, most composites have non-periodic structure with practically random geometry (Batdorf, 1978; Batdorf and Ghaffarian, 1984).

Randomness in composite geometry occurs also on its micro-scale. This results mainly from the structure of molecular matter, natural macroscopic heterogeneity (porosity and inclusions), technological inaccuracies (debonding of fiber surface from surrounding matrix) or degradation of component materials (ageing and fatigue processes) (Kelly, 1989; Moavenzadeh, 1990). For many years these uncertainties have been approximated by the stochastic nature of elastic properties; this idea first appeared at the beginning of the 1960s (Beran, 1968; Christensen, 1979).

In general, probabilistic models in composite materials theories have been connected mainly with statistical theories of their strength (Phoenix and Smith, 1983; Phoenix and Tierney, 1983; Zweben and Rosen, 1970), Dyson and Bethe–Salpether hierarchical equations (Sobczyk, 1982) and the derivation of the effective properties (Arminjon, 1991; Ostoja-Starzewski and Wang, 1989) and bounds of these properties (Avellaneda, 1987). Because of this fact numerical investigations have been based on Monte-Carlo simulations only and have been applied to the problem of critical crack size (Barry, 1978) and homogenization problems (Kamiński, 1996; Sab, 1992).

However, there are many other probabilistic methods in computational mechanics. In addition to Monte-Carlo simulation the following approaches are available, for example: Fisher's theory of experiments (Fisher, 1971), stratified sampling and Latin hypercube sampling (Liu *et al.*, 1986) or the stochastic finite element method (SFEM) (Hien, 1990; Kleiber and Hien, 1992; Liu *et al.*, 1986) which was recently proposed for composite behavior modeling in Kamiński and Gajl (1995).

It is well known that mechanical properties of a composite depend on the properties of its constituents and on their interaction. The most important technological problems connected with the fiber composites are the interfacial microcracks (resulting from thermal

incompatibility of composite constituents), interfacial stress concentrations and degradation mechanisms. In most environments composites absorb water, which can break the interfacial bonds between fiber and matrix and lead to the reduction of load transfer and worsening of the overall mechanical properties of the structure. Water penetration can cause swelling and plastification of the matrix, and capillary tubes along the fiber–matrix interface can then occur. The presence of water on the fiber–matrix boundary leads to further degradation of the fiber and generates microcracks with water penetration extending deeper in the direction parallel to the fiber orientation. The phenomena described above may lead to interphase debonding, interfacial sliding and even to fiber pull-out.

The internal geometry of the stochastic composite is the basic difficulty in the development of analytical expressions for the elastic constants. This problem has been approached in a number of ways (Ashton *et al.*, 1969; Christensen, 1979; Hashin, 1972; Sendeckyj, 1974) using bounding methods for elastic properties (Hashin, 1965; Hashin and Shtrikman, 1963; Hill, 1964; Milton and Kohn, 1988), special models, for example the composite cylinder assemblage (Christensen, 1979; Hashin, 1972), and Halpin–Tsai equations (Ashton, 1969). Nowadays, the most popular micromechanical approaches to homogenization problems are direct particle interaction methods (Chang *et al.*, 1995; Chen and Acrivos, 1978) and "effective medium methods" such as:

- simplified mechanics of materials type equations (cf. Caruso and Chang, 1995);
- fiber substructuring model (cf. Murthy and Chamis, 1992);
- vanishing fiber-diameter model (cf. Bahei-El-Din *et al.*, 1981);
- self-consistent model (Budiansky, 1965; Hill, 1964);
- Mori–Tanaka model (Benveniste *et al.*, 1990; Mori and Tanaka, 1973);
- methods of cells (cf. Aboudi, 1991).

In practice this problem is much more complicated because matrices are often made of viscoelastic or plastic materials (Kelly, 1989; Moavenzadeh, 1990) and description of the nonlinear behavior is complex even for simple loading conditions (Adams, 1970; Dvorak and Rao, 1976). Uncertainties in microgeometry interface in nonlinear problems are also very important with respect to such aspects as localization of plastic zones (Drucker, 1975; Dvorak and Rao, 1976), thermomechanical effects and composite failure criteria (Tsai and Wu, 1971). It would therefore seem important to determine in what way the stochastic interface between both composite phases influences the composite behavior. An analysis of this problem will be performed here using the example of a plane section of a periodic fiber composite with a square periodicity cell and a centrally located fiber with a circular cross-section. The fibers are long, unidirectionally aligned and deterministically located within the composite. Random varying elastic properties of the constituents are assumed and the matrix is considered to be brittle. As has been shown by computational simulations (Noor and Shah, 1993) fiber composites show the highest sensitivity to changes of elastic properties in this plane. The results presented by Kamiński (1995) demonstrated that in the range of linear-elastic behavior, with discontinuities properly located on the fiber–matrix boundary and for the proper parameters of these discontinuities, it is possible that both the phases will locally debond. With further increase of external load we have a completely different primary geometry of the nonlinear problem, thus we can obtain qualitatively and quantitatively different results.

In numerical modeling of contact problems the statistical parameters of the contact zone (interphase) discontinuities are usually replaced with deterministic correctors. As a result a new nonlinear constitutive relation is established for the contact region (Mital *et al.*, 1993; Wriggers and Zavarise, 1993; Zavarise *et al.*, 1992a; Zavarise *et al.*, 1992b). This deterministic approximation has been mainly due to the lack of proper stochastic numerical tools. Independently from the contact formulations, the interphase defect models were developed. One of the first approaches was the "spring-layer model" employed by Benveniste (1985) and Hashin (1990). The effect of a sliding interface on the elastic properties of random composites was investigated by Jasiuk *et al.* (1992), while the effect of interphase flaws and matrix cracks on these properties was studied by Achenbach and Choi (1979) and Choi and Achenbach (1995). In homogenization problems variational inequalities have

also been used for deterministic analysis of interface discontinuities and microcracks (Gajl, 1990; Telega, 1988). Methods applied in the above-mentioned formulations do not, however, enable one to obtain stochastic characterization of displacement and stress fields.

From the point of view of the degradation phenomena in a composite structure, as described above, we can assume that there are "bubbles" occurring in the contact zone of the matrix region (cf. Kaminski, 1995). These "bubbles" were considered for the first time in micro-mechanical approaches to the contact problems cited above. They are located on the contact surface, with some "teeth" with sharp sides directed towards the geometric centre of the fiber, which technologically occur for example in the superconducting coils in the corresponding fiber zone. We further assume that the sizes of these "bubbles" and "teeth", as well as the frequency of their occurrence on the fiber circumference in a periodicity cell, are random variables with a Gaussian distribution. The regions containing the random discontinuities will be separated geometrically in both phases and then replaced with homogenized materials. The problem of linear elasticity defined in the region with stochastic geometry (difficult even for numerical analysis) will be replaced by an equivalent problem with deterministic geometry with randomly varying elastic properties, which will be analysed numerically using the SFEM. Due to this it will be possible to consider the correlation of the elastic properties in the region of the given material and in the contact zone within the material, and also to obtain as a final result the first two probabilistic moments of the displacement field and the expected values of the stress tensor.

2. MATHEMATICAL INTERFACE DEFECTS MODEL

2.1. *Problem formulation*

Let us suppose that $Y \subset \Omega^2$ is a periodic two-phase linear-elastic composite structure with randomly varying elastic properties in an undeformed and unstressed state (Kamiński, in press), where Ω is a periodicity cell of Y, Ω_1 is the fiber region and Ω_2 is the matrix region (Fig. 1).

Next we assume that Ω is a bounded simple-connected region uniplanar with the $x_3 = 0$ plane, and having two perpendicular symmetry axes. Let Ω_1 and Ω_2 be disjoint coherent regions such that $\Omega = \Omega_1 \cup \Omega_2$ containing linear-elastic transversely isotropic homogeneous media.

Let Young's modulus $e = e(x)$ be a Gaussian random variable, $e(x) = e(x; \omega)$, where $x \in \Omega; \omega \in S$, where S is an additional probability space and the expected values vector is defined as follows:

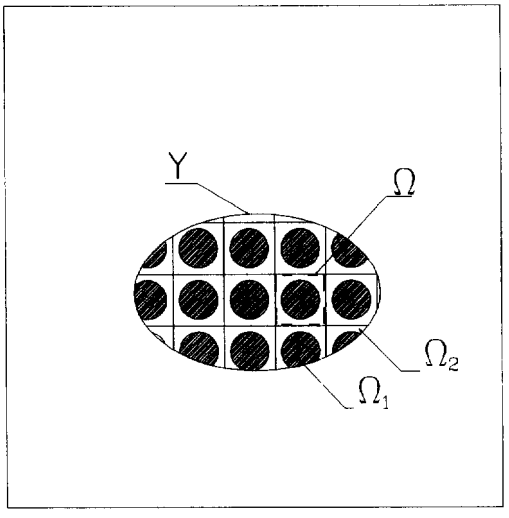

Fig. 1. The periodicity cell of fiber composite structure.

$$\mathbf{E}(e(x)) = \begin{bmatrix} \mathbf{E}(e_1)\,; x \in \Omega_1 \\ \mathbf{E}(e_2)\,; x \in \Omega_2 \end{bmatrix}, \tag{1}$$

with a covariance matrix

$$\operatorname{cov}(e_i, e_j) = \begin{bmatrix} \operatorname{var}(e_1) & \mathbf{0} \\ \mathbf{0} & \operatorname{var}(e_2) \end{bmatrix}, \tag{2}$$

where $\operatorname{cov}(e_1, e_2) = 0$ due to the lack of correlation of random functions describing the elastic properties in the Ω_1 and Ω_2 regions, which can be justified from the physical point of view.

The Poisson's ratio is assumed to be a deterministic function so that

$$v(x) = \begin{bmatrix} v_1\,; x \in \Omega_1 \\ v_2\,; x \in \Omega_2 \end{bmatrix}. \tag{3}$$

Let us define the random elasticity tensor field $C_{ijkl}(x\,;\omega)$:

$$C_{ijkl}(x\,;\omega) = e(x\,;\omega)\left\{\delta_{ij}\,\delta_{kl}\frac{v(x)}{(1+v(x))(1-2v(x))} + (\delta_{ik}\,\delta_{jl} + \delta_{il}\,\delta_{jk})\frac{1}{2(1+v(x))}\right\}, \tag{4}$$

where $i, j, k, l = 1, 2$.

With the elastic properties in Ω so defined we seek a random displacement field $u_i(x\,;\omega)$ and a random stress tensor $\sigma_{ij}(x\,;\omega)$ satisfying the following boundary-value problem:

$$\sigma_{ij}(x\,;\omega) = C_{ijkl}(x\,;\omega)\varepsilon_{kl}(x\,;\omega), \tag{5}$$

$$\varepsilon_{ij}(x\,;\omega) = \frac{1}{2}\left(\frac{\partial u_i(x\,;\omega)}{\partial x_j} + \frac{\partial u_j(x\,;\omega)}{\partial x_i}\right), \tag{6}$$

$$\sigma_{ij,j}(x\,;\omega) = 0, \tag{7}$$

$$u_i(x\,;\omega) = \bar{u}_i(x\,;\omega)\,; \quad \in \partial\Omega_u, \tag{8}$$

$$\sigma_{ij}(x\,;\omega) = \bar{\sigma}_{ij}(x\,;\omega)\,; \quad \in \partial\Omega_\sigma. \tag{9}$$

2.2. *Homogenization of contact zones*

Let us assume a contact between the linear-elastic transversely isotropic regions $\Omega_1 \subset \Re^2$ and $\Omega_2 \subset \Re^2$ on the $\partial\Omega_{12}$ interface (Fig. 2). The stochastic elastic behavior of these

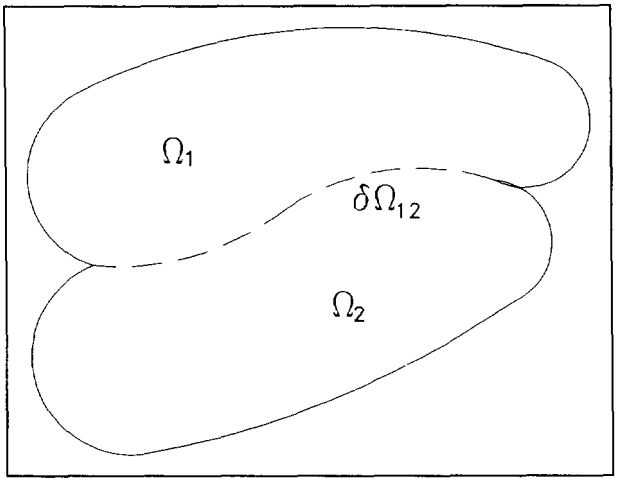

Fig. 2. Macro-geometry of the interphase boundary.

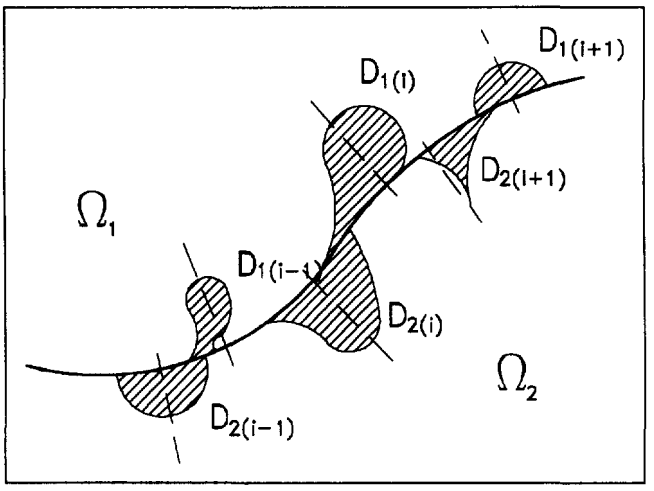

Fig. 3. Stochastic defects on the interphase boundary.

regions is uniquely characterized by the first two moments of the Young's modulus and the deterministic function of the Poisson's ratio.

Next, let us assume that there are discontinuities with random volume and frequency and that these are Gaussian variables on $\partial\Omega_{12}$. We will assume that each of these discontinuities has a continuous boundary (cf. Fig. 3).

Let D_1 and D_2 denote the total area of these discontinuities in Ω_1 and Ω_2

$$D_1 = \bigcup_{i=1}^{n} D_{1(i)}; \quad D_2 = \bigcup_{i=1}^{n} D_{2(i)}.$$

We will establish regions $C_1 \subset \Omega_1$ and $C_2 \subset \Omega_2$ such that, with probability equal to 1, $D_1 \subset C_1$ and $D_2 \subset C_2$. For this purpose let us introduce random functions $\Delta_{j(i)}(x;\omega)$ where $j = 1, 2$ such that:

$$\Delta_{j(i)}(x;\omega) = \sup_{D_{j(i)}} \{|\mathbf{AB}| : A \in \partial\Omega_{12}, B \in D_{j(i)} \wedge \mathbf{AB} \perp \partial\Omega_{12}\}. \tag{10}$$

Because of the assumed continuity along the $D_{j(i)}$ boundary there exist expected values and variances of $\Delta_{j(i)}(x;\omega)$. In addition let us define

$$\Delta_{jc} = E[\Delta_j(x;\omega)] + 3\sqrt{\operatorname{var}[\Delta_j(x;\omega)]}. \tag{11}$$

It is easy to prove that C_j can be expressed in the following form:

$$C_j = \{P'(x,y) \in \Omega_j; d(P', \partial\Omega_{jk}) \leqslant \Delta_{jc}\}. \tag{12}$$

To replace the contact problem in regions Ω_1 and Ω_2 with an equivalent stochastic problem of elasticity theory we can average the elasticity constants $e(x;\omega)$ and $\nu(x)$ in the regions C_j. To do this we use the homogenization method. According to this method the effective property $Y^{(\text{eff})}$ characterizing the homogenized region Ω is an adequate average of the Y_i properties defined on continuous, coherent subsets Ω_i of Ω such that

$$\Omega = \bigcup_{i=1}^{n} \Omega_{(i)}.$$

In the deterministic case this average is described by the equation

$$Y^{(\mathrm{eff})} = \frac{\sum_i Y_i(x) \cdot \Omega_i}{|\Omega|}; x \in \Omega, \tag{13}$$

where $|\Omega|$ is the two-dimensional Lesbegue measure of Ω. Let us assume that $|\Omega|$ is a deterministic variable. Thus, the first two moments of $Y^{(\mathrm{eff})}(\omega)$ variable can be calculated for the contact problem from the following equations:

$$\mathbf{E}[Y^{(\mathrm{eff})}(\omega)] = \frac{1}{|\Omega|} \sum_i \mathbf{E}[Y_i(x;\omega)]\mathbf{E}[\Omega_i(\omega)]; x \in \Omega, \tag{14}$$

$$\mathrm{var}[Y^{(\mathrm{eff})}(\omega)] = \frac{1}{|\Omega|^2} \sum_i \mathrm{var}[Y_i(x;\omega)]\mathrm{var}[\Omega_i(\omega)]; x \in \Omega, \tag{15}$$

which result from the lack of correlation of Ω_i and the function Y_i defined on Ω_i.

In this way the characterized homogenization (averaging) of contact zones on Ω, for all distributions of discontinuities with the same number and frequency gives the same probabilistic output of $Y^{(\mathrm{eff})}(\omega)$. Thus in the composite periodicity cell with averaged interphase we may analyse only a quarter of this cell.

2.3. *Homogenization of matrix contact zone*

Let us suppose that there is a finite number of discontinuities in the matrix region located on the fiber–matrix interface. These discontinuities are approximated as "bubbles" (Kamiński, 1995) with their diameters placed on the interface (Fig. 4). The random distribution of the assumed defects is uniquely defined by the expected values and variances of the frequency and radius of the "bubbles". As shown below, there is a sufficient number of parameters to obtain a complete characterization of the contact zone averaged elastic constants (Fig. 5).

Using eqns (14) and (15) we can establish the expected value and the variance of the effective Young's modulus e_k, the terms which are missing in the covariance matrix of this modulus and also the Poisson's ratio. The expected value can be derived as

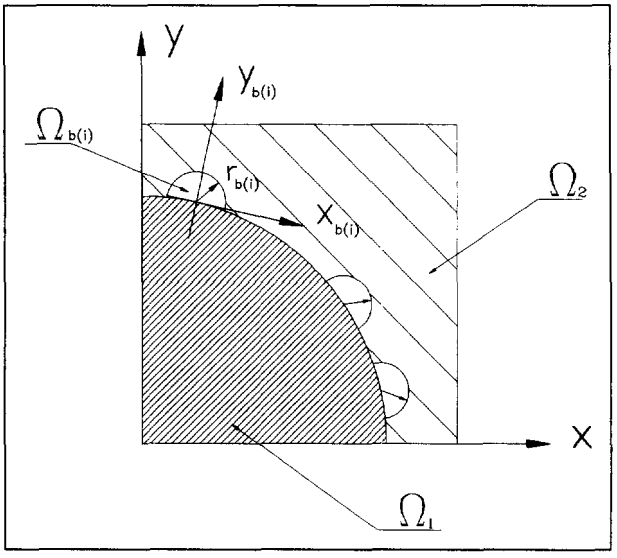

Fig. 4. Stochastic interphase defects in the matrix region.

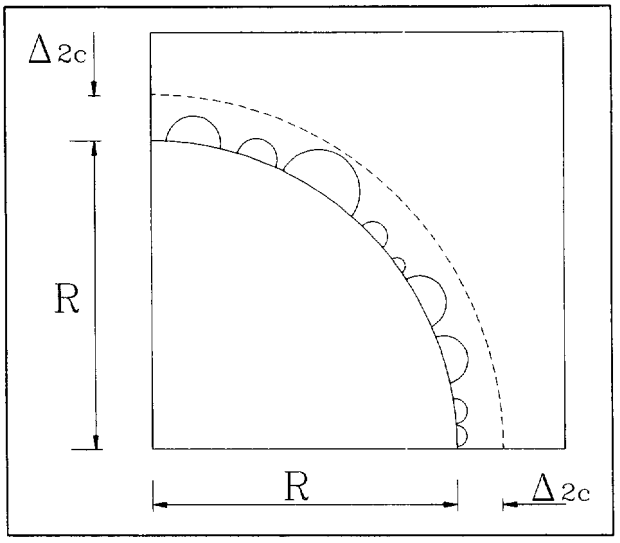

Fig. 5. The contact zone in the matrix region.

$$\mathbf{E}[e_{2c}] = \mathbf{E}\left[\frac{S_{\Omega_{2c}} - S_b}{S_{\Omega_{2c}}} \cdot e_2\right] = \mathbf{E}[e_2] \cdot \left(1 - \frac{1}{S_{\Omega_{2c}}} \cdot \mathbf{E}[S_b]\right). \tag{16}$$

As it can be easily seen in the above relation we have

$$S_{\Omega_{2c}} = \Pi\left\{(R + \mathbf{E}[r_{\bar{\Omega}}] + 3\sqrt{\operatorname{var}[r_{\bar{\Omega}}]})^2 - R^2\right\}. \tag{17}$$

In a similar way we obtain the variance as

$$\operatorname{var}[e_{2c}] = \operatorname{var}\left[\left(1 - \frac{S_b}{S_{\Omega_{2c}}}\right) \cdot e_2\right]. \tag{18}$$

This equation can be transformed to the following form (see Kamiński, 1995),

$$\operatorname{var}[e_{2c}] = \left\{1 - \frac{1}{S_{\Omega_{2c}}} \mathbf{E}[S_b]\right\}^2 \cdot \operatorname{var}[e_2] + \frac{1}{S^2_{\Omega_{2c}}} \operatorname{var}[S_b] \cdot \operatorname{var}[e_2] + \frac{1}{S^2_{\Omega_{2c}}} \operatorname{var}[S_b] \cdot \mathbf{E}^2[e_2], \tag{19}$$

which, neglecting moments of higher than second order, can be reduced to

$$\operatorname{var}[e_{2c}] = \left\{1 - \frac{1}{S_{\Omega_{2c}}} \mathbf{E}[S_b]\right\}^2 \cdot \operatorname{var}[e_2] + \frac{1}{S^2_{\Omega_{2c}}} \operatorname{var}[S_b] \cdot \mathbf{E}^2[e_2]. \tag{20}$$

Now the distribution parameters S_b have to be found. There holds

$$S_b = \tfrac{1}{2}\Pi(r_b)^2 M_b, \tag{21}$$

where M_b is the number of $\Omega_{b(i)}$ regions in Ω_{2c} equal to

$$M_b = 2\Pi R m_b. \tag{22}$$

Therefore, we have

$$\mathbf{E}[M_b] = 2\Pi R \cdot \mathbf{E}[m_b] \tag{23}$$

and

$$\text{var}\,[M_b] = 4\Pi^2 R^2 \cdot \text{var}\,[m_b]. \tag{24}$$

From the definition of expected value we obtain

$$\mathbf{E}[S_b] = \frac{\Pi}{2} \cdot \mathbf{E}[(r_b)^2 M_b] = \frac{\Pi}{2} \cdot \{\mathbf{E}^2[r_b] + \text{var}\,[r_b]\} \cdot \mathbf{E}[M_b]. \tag{25}$$

Finally, we find the variance of S_b as

$$\text{var}\,[S_b] = \text{var}\left[\frac{\Pi}{2}(r_b)^2 M_b\right] = \frac{\Pi^2}{4}\text{var}\,[(r_b)^2 M_b]. \tag{26}$$

It can be shown that this expression may be transformed into the form

$$\text{var}\,[S_b] = \frac{\Pi^2}{4}(E^2[r_b] + \text{var}\,[r_b])^2 \cdot \text{var}\,[M_b]$$
$$+\frac{\Pi^2}{2}\text{var}\,[r_b] \cdot (E^2[M_b] + \text{var}\,[M_b]) \cdot (2E^2[r_b] + \text{var}\,[r_b]). \tag{27}$$

By substituting the equations describing the S_b distribution parameters into the relations describing expected value and variance of the e_k modulus distribution we can similarly derive the data necessary for the numerical analysis.

It should be observed that by homogenizing the Poisson's ratio in Ω_k we obtain

$$\nu_{2c} = \left(1 - \frac{\mathbf{E}(S_b)}{S_{\Omega_{2c}}}\right) \cdot \nu_2. \tag{28}$$

2.4. *Homogenization of fiber contact zone*

By arguments similar to those given in Section 2.3, in order to carry out the averaging process over the contact zone we have to approximate the random defects on the fiber side of composite interface by a sequence of simple geometrical forms. Let us therefore assume a finite number of these discontinuities is added to the contact zone. The fiber material has good (much better than the matrix) resistance to degradation (Christensen, 1979; Kelly, 1989; Moavenzadeh, 1990) and so we approximate defects in the Ω_1 region as "teeth" with their "sharp" sides directed towards the fiber centre. A single discontinuity is made by complementing of a two circle quarters to a rectangle (Figs 6 and 7).

As in the previous case we have

$$\mathbf{E}[e_{1c}] = \mathbf{E}[e_1] \cdot \left(1 - \frac{1}{S_{\Omega_{1c}}} \cdot \mathbf{E}[S_i]\right) \tag{29}$$

and

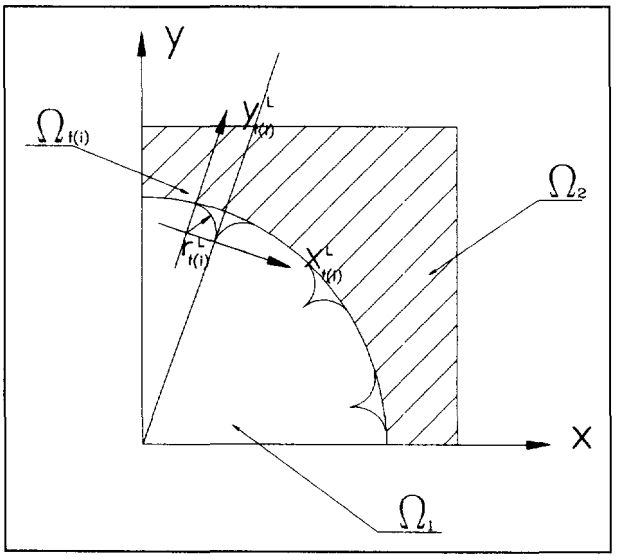

Fig. 6. Stochastic interphase defects in the fiber region.

$$\mathrm{var}\,[e_{1c}] = \left\{1 - \frac{1}{S_{\Omega_{1c}}}\mathbf{E}[S_t]\right\}^2 \cdot \mathrm{var}\,[e_1] + \frac{1}{S^2_{\Omega_{1c}}}\mathrm{var}[S_t] \cdot \mathrm{var}\,[e_1] + \frac{1}{S^2_{\Omega_{1c}}}\mathrm{var}\,[S_t] \cdot \mathbf{E}^2[e_1]. \tag{30}$$

The relations describing the discontinuity parameters will have a different form

$$S_t = \left(2 - \frac{\Pi}{2}\right)(r_t)^2 M_t, \tag{31}$$

so that

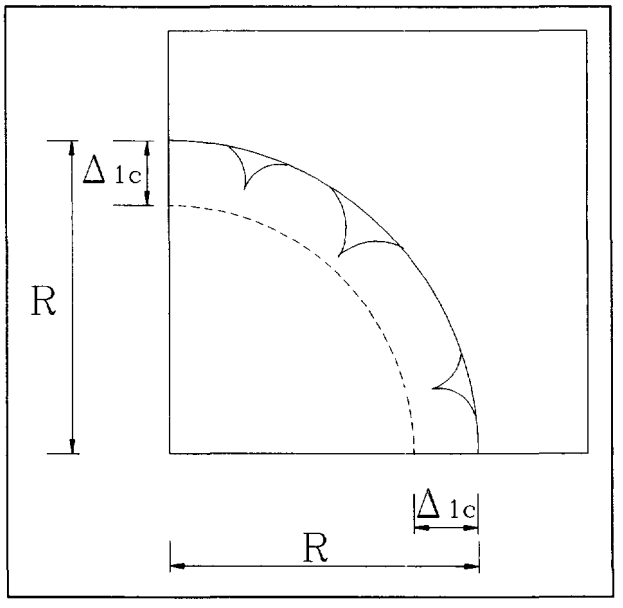

Fig. 7. The contact zone in the fiber region.

$$\mathbf{E}[S_t] = \left(2 - \frac{\Pi}{2}\right) \cdot \mathbf{E}[(r_t)^2 M_t] = \left(2 - \frac{\Pi}{2}\right) \cdot \{\mathbf{E}^2[r_t] + \text{var}[r_t]\} \cdot \mathbf{E}[M_t], \tag{32}$$

and finally

$$\text{var}[S_t] = \left(2 - \frac{\Pi}{2}\right)^2 (\mathbf{E}^2[r_t] + \text{var}[r_t])^2 \cdot \text{var}[M_t]$$

$$+ 2 \cdot \left(2 - \frac{\Pi^2}{2}\right)^2 \cdot \text{var}[r_t] \cdot (\mathbf{E}^2[M_t] + \text{var}[M_t]) \cdot (2\mathbf{E}^2[r_t] + \text{var}[r_t]). \tag{33}$$

The Poisson's ratio in the contact region associated with the fiber is then given by

$$\nu_{1c} = \left(1 - \frac{\mathbf{E}(S_t)}{S_{\Omega_{1c}}}\right) \cdot \nu_1. \tag{34}$$

Finally, the covariance matrix of Young's modulus in the Ω region takes the following form:

$$\text{cov}(e^{(i)}, e^{(j)}) = \begin{bmatrix} \text{var}[e_1] & \text{cov}[e_1, e_{1c}] & \mathbf{0} & \mathbf{0} \\ \text{cov}[e_1, e_{1c}] & \text{var}[e_{1c}] & \mathbf{0} & \mathbf{0} \\ \mathbf{0} & \mathbf{0} & \text{var}[e_{2c}] & \text{cov}[e_{2c}, e_2] \\ \mathbf{0} & \mathbf{0} & \text{cov}[e_{2c}, e_2] & \text{var}[e_2] \end{bmatrix}. \tag{35}$$

Zeroing of the corresponding covariance matrix can be achieved on the basis of the assumed mutual independence of Young's modulus random variables within the fiber, its contact zone and its associated regions within the matrix.

3. NUMERICAL ANALYSIS

3.1. *Computational implementation*

Denoting the random variable of this problem (i.e. the Young's modulus) as a vector $\{b^r(x;\omega)\}$ and its probability densities by $g(b^r)$ and $g(b^r, b^s)$, respectively, $r, s = 1, 2 \ldots, R$, we can define the expected values as:

$$\mathbf{E}[b^r] = \int_{-\infty}^{+\infty} b^r g(b^r)\, \mathrm{d}b^r, \tag{36}$$

and the covariances as

$$\text{cov}(b^r, b^s) = \int_{-\infty}^{+\infty} \int_{-\infty}^{+\infty} (b^r - \mathbf{E}[b^r])(b^s - \mathbf{E}[b^s]) g(b^r, b^s)\, \mathrm{d}b^r\, \mathrm{d}b^s. \tag{37}$$

Generally the variational formulation, equivalent to the previously derived equation system (5)–(9), obtained from the Hamilton's Theorem leads to the following algebraic system of equations (Hien, 1990; Kleiber and Hien, 1992; Liu *et al.*, 1986):

$$\mathbf{K}^0 \mathbf{q}^0 = \mathbf{Q}^0, \tag{38}$$

$$\mathbf{K}_0 \mathbf{q}^r = \mathbf{Q}^r - \mathbf{K}^r \mathbf{q}^0, \tag{39}$$

$$\mathbf{K}^0\mathbf{q}^{(2)} = \tfrac{1}{2}[\mathbf{Q}^{,rs} - 2\cdot\mathbf{K}^{,r}\mathbf{q}^{,s} - \mathbf{K}^{,rs}\mathbf{q}^0]\,\mathrm{cov}(b^r, b^s), \tag{40}$$

where

$$\mathbf{q}^{(2)} = \tfrac{1}{2}\mathbf{q}^{,rs}\,\mathrm{cov}(b^r, b^s) \tag{41}$$

and $1 \leqslant r, s \leqslant R$ (R—the total number of the random vector components). Zeroth order functions from the FEM equations are denoted by $(.)^0$ and $(.)^{,r}$, $(.)^{,rs}$—the first and the second partial derivatives with respect to the random variables. $\mathbf{K}, \mathbf{q}$ and $\mathbf{Q}$ denote the global stiffness matrix displacement and external load vectors, respectively. It is easy to prove (Kamiński and Gajl, 1995) that the algebraic equation system (38)–(40) reduces to:

$$\mathbf{K}^0\mathbf{q}^0 = \mathbf{Q}^0, \tag{42}$$

$$\mathbf{K}^0\mathbf{q}^{,r} = -\mathbf{K}^{,r}\mathbf{q}^0, \tag{43}$$

$$\mathbf{K}^0\mathbf{q}^{(2)} = -2\cdot\mathbf{K}^{,r}\mathbf{q}^{,s}\,\mathrm{cov}(b^r, b^s). \tag{44}$$

In the above equations we compute successively $\mathbf{q}^0$ from the first, $\mathbf{q}^{,r}$ from the second and $\mathbf{q}^{,rs}$ from the last equation and then derive the expected values of the displacement as

$$\mathbf{E}[q_\beta] = q_\beta^0 + \tfrac{1}{2}q_\beta^{,rs}\,\mathrm{cov}(b^r, b^s) = q_\beta^0 + q_\beta^{(2)} \tag{45}$$

and its covariances

$$\mathrm{cov}(q_\alpha^r, q_\beta^s) = q_\alpha^{,r} q_\beta^{,s}\,\mathrm{cov}(b^r, b^s). \tag{46}$$

The expected values of the stress tensor in the finite element e are given by

$$\mathbf{E}[\sigma_{ij}^e] = C_{ijkl}^{0(e)} B_{kl\alpha}^{(e)} q_{\alpha(e)}^0 + \tfrac{1}{2}[2C_{ijkl}^{,r(e)} q_{\alpha(e)}^{,s} + C_{ijkl}^{0(e)} q_{\alpha(e)}^{,rs}] B_{kl\alpha}^{(e)}\,\mathrm{cov}(b^r, b^s). \tag{47}$$

The general purpose of the numerical analysis is to test the stochastic elastic behavior of a fiber composite when the Young's moduli of the component materials are random variables and there are stochastic discontinuities localized on the interface of both phases of this composite. Moreover, numerical tests are carried out to establish the sensitivity of the averaged elastic constants with respect to the frequency of interface defects and the volume in a periodicity cell quarter.

The finite element discretization used in the computational tests is shown in Fig. 8 and 9—a quarter model with smaller contact zones in the upper figure and with larger ones in the lower one. This example (without the interface analysis) has been analysed previously (cf. Kamiński, 1996).

The numerical implementation enabling these computations is based on the 4th nodes isoparametric rectangular plane element of the POLSAP system (Bathe *et al.*, 1973; Hien, 1990). The auxiliary procedures required to average Young's modulus and Poisson's ratio can easily be incorporated into the POLSAP system as a special purpose Interface Stochastic Plane Element. The composite structure is subjected to uniform tension on the vertical cell boundary (60 finite elements with 176 d.f.); the plane strain element with unit thickness is used. Six numerical tests have been performed assuming small and large contact zones on both sides of the interface, with different values of discontinuity frequency (in turn: 0%, 25% and 50%). In each, the first two moments of the displacement function are observed on the phase boundary and on the vertical edge subjected to tension, and the coefficient of variation of displacements is given by the formula

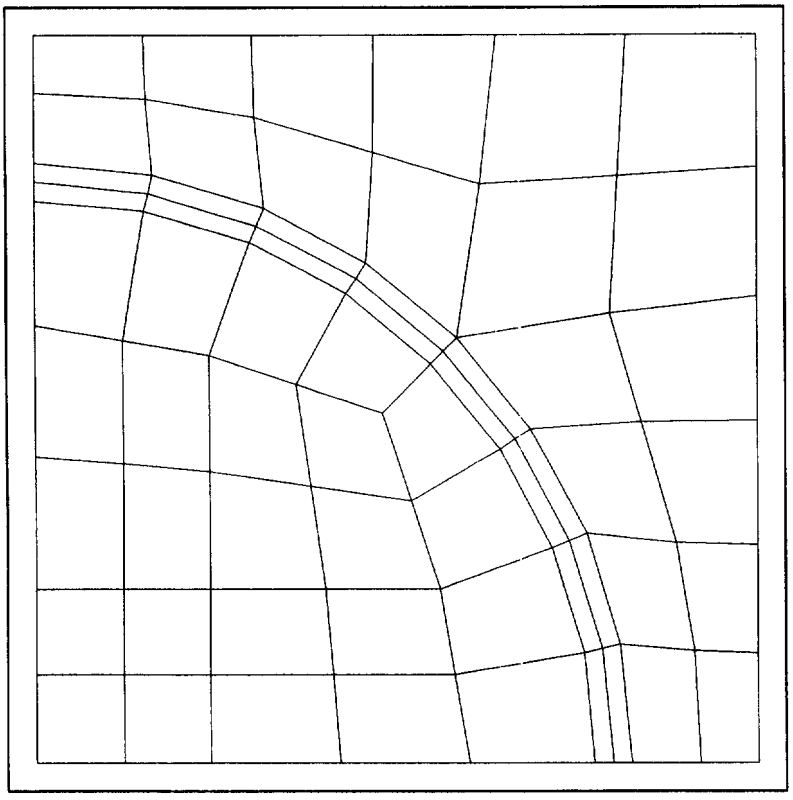

Fig. 8. Discretization of fiber composite with smaller contact zone.

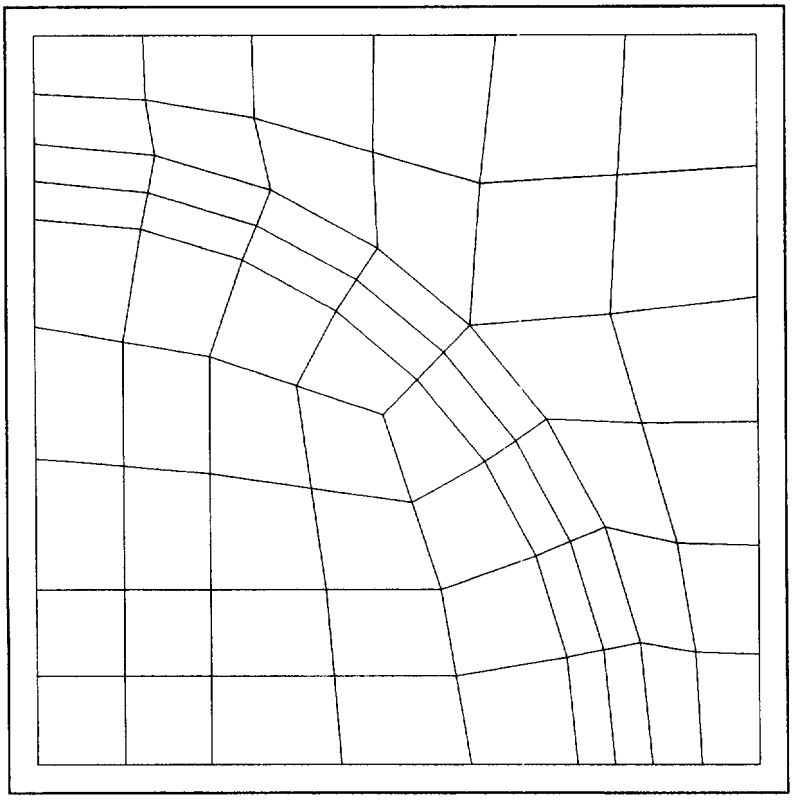

Fig. 9. Discretization of fiber composite with greater contact zone.

$$\alpha[b(x;\omega)] = \frac{\sqrt{\text{var}\,[b(x;\omega)]}}{\mathbf{E}^2[b(x;\omega)]}. \tag{48}$$

The material properties of fiber and matrix are taken as follows: $\mathbf{E}(e_1) = 84.0$ GPa, $v_1 = 0.22$, $\sigma(e_1) = 4.2$ GPa, $\mathbf{E}(e_2) = 4.0$ GPa, $\sigma(e_2) = 0.4$ GPa, $v_2 = 0.34$ (expected values and standard deviations of the Young's modulus and Poisson's ratio, respectively).

3.2. *Results and discussion*

First, the influence of the interface discontinuity parameters (radius and frequency) on the effective elastic parameters of the contact zones is analysed. For this purpose the FORTRAN subroutine which computes expected values and variations of the averaged Young's modulus and Poisson's ratio value was implemented. In numerical tests we assume the number of the interface discontinuities in the matrix and fiber contact zone as 4, 10, 20 and 40 with the width of the observed contact region varying between 4.0×10^{-3} and 2.0×10^{-2}. The results of these computations are presented in Figs 10–15: the expected values of the homogenized Young's modulus functions are given in Figs 10 and 11, the averaged Poisson's ratio functions in Figs 12 and 13 and the variances of the Young's modulus functions in Figs 14 and 15. All of these variables are marked, respectively, on the vertical axis; on the horizontal axis the expected value of the radius of the interface defects is given.

As one may expect, the resulting expected values of the homogenized Young's modulus in both the matrix and the fiber regions (and similarly for the Poisson's ratio) are linear functions of the contact zone widths. The variances of the averaged Young's modulus are non-linear functions of this variable, and its non-linearity is directly dependent on the number of interface defects.

Comparing Figs 10 and 11 with Figs 14 and 15 it can be seen that the Young's modulus in the matrix contact zone is, for the present problem, much more sensitive to variation in its parameters than the same modulus in the fiber contact zone. This is implied by the greater coefficient of variation in the matrix region than in the fiber. On the other hand, homogenized elastic properties are derived by averaging their values in both the regions. Thus in the matrix, because of the larger volume of "bubbles" compared to fiber "teeth", greater changes in these properties can be expected.

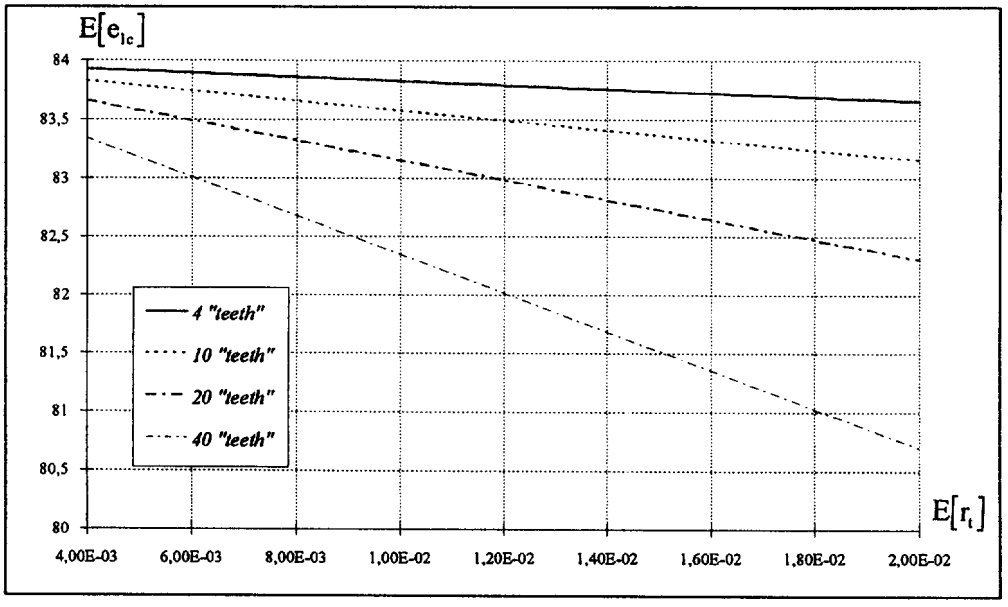

Fig. 10. Expected values of homogenized Young's modulus in fiber region.

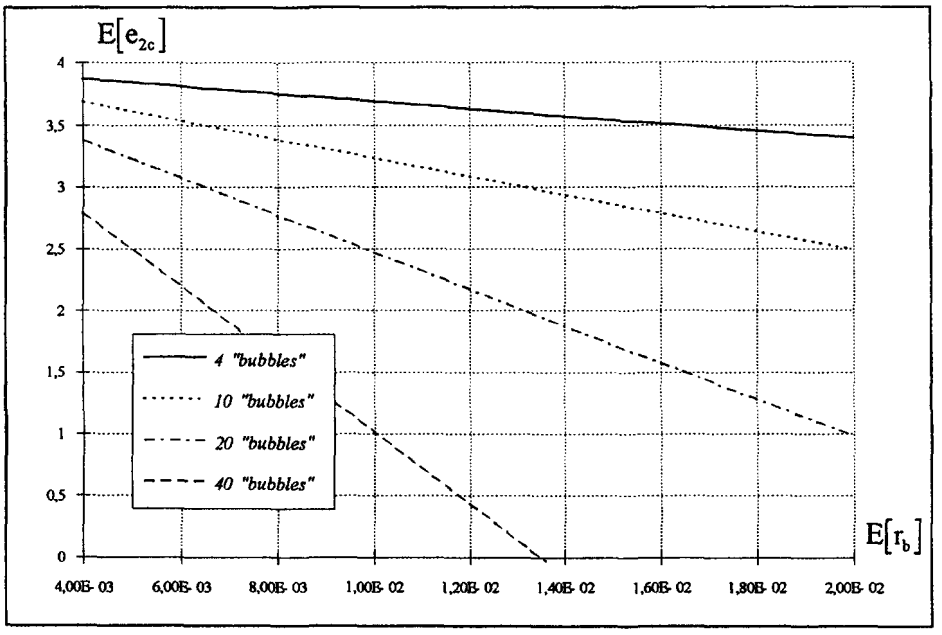

Fig. 11. Expected values of homogenized Young's modulus in matrix region.

Another interesting effect (cf. Figs 14 and 15) is the increase in the variances of the homogenized Young's modulus in the matrix contact zone for increasing width of this zone and the number of "bubbles". The reverse effect occurs for the fiber side of the interface and its "teeth". This is due to the fact that "bubbles" occupy more than half of the volume of the corresponding contact zone, and "teeth" less than half.

Next, the probabilistic displacement state in the composite phases interface and tensioned edge is analysed. The expected values of the displacements or their coefficients of variation are placed on the vertical axes of all figures. The β angle which determines the

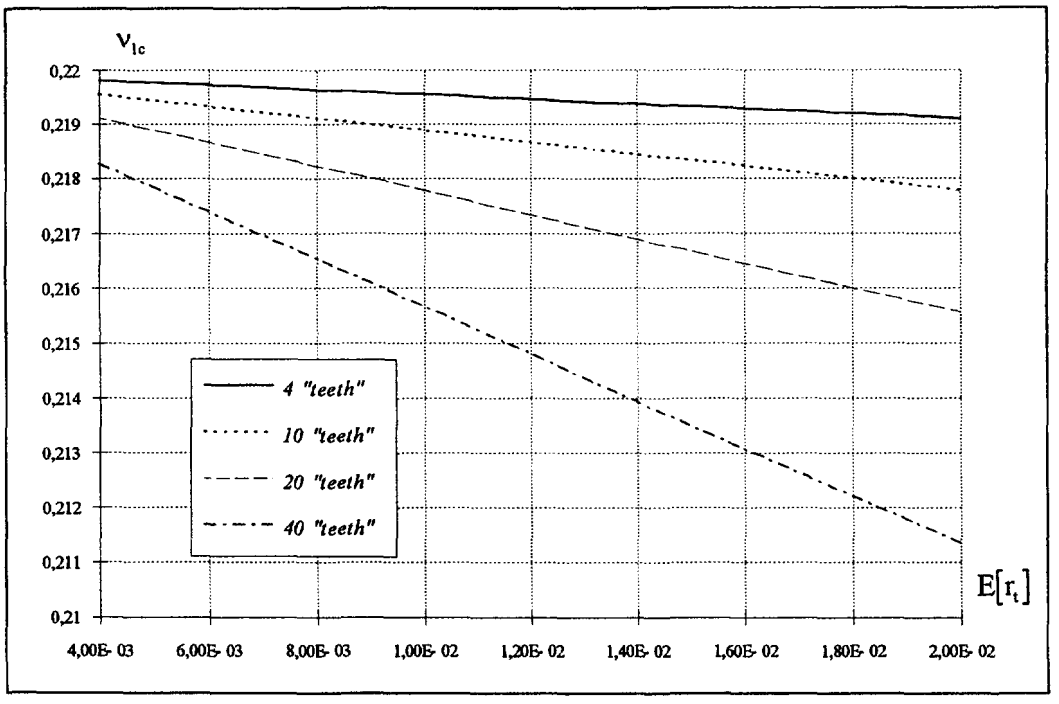

Fig. 12. Homogenized Poisson's ratio in fiber region.

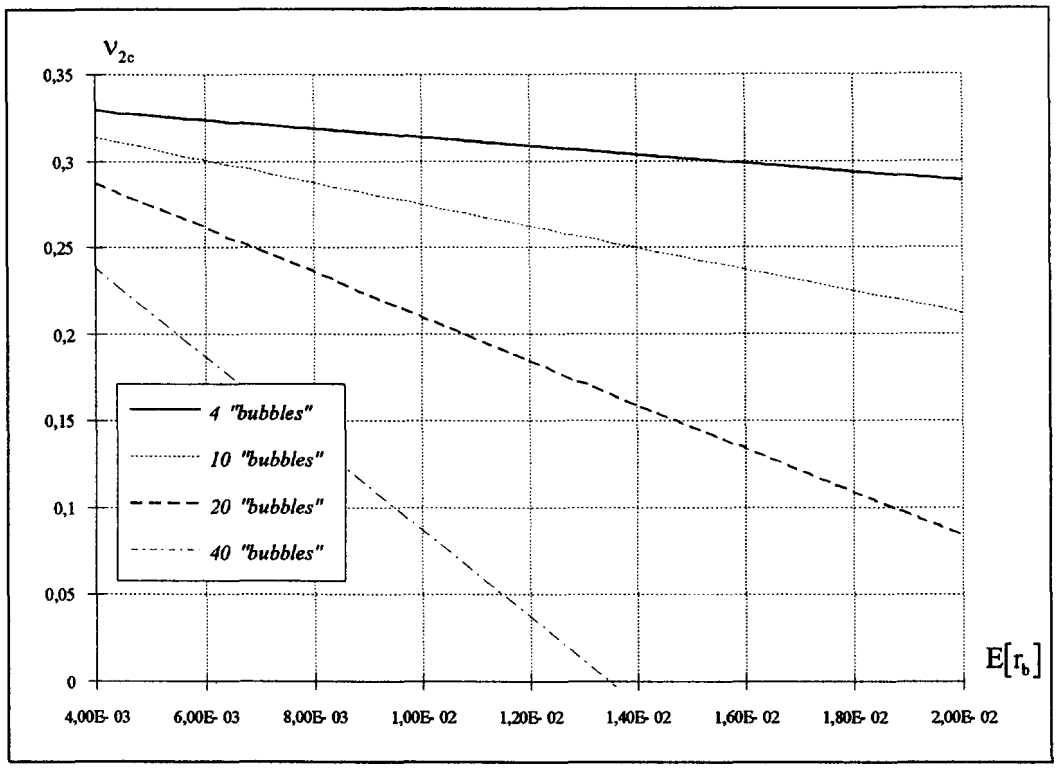

Fig. 13. Homogenized Poisson's ratio in matrix region.

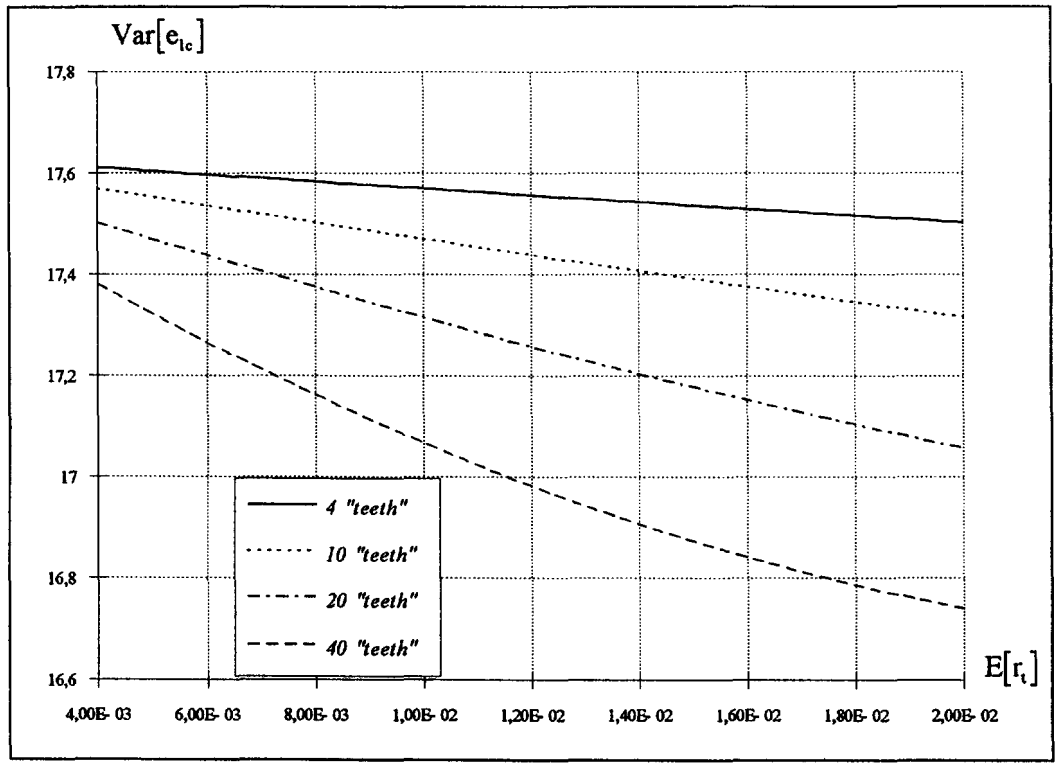

Fig. 14. Variances of homogenized Young's modulus in fiber region.

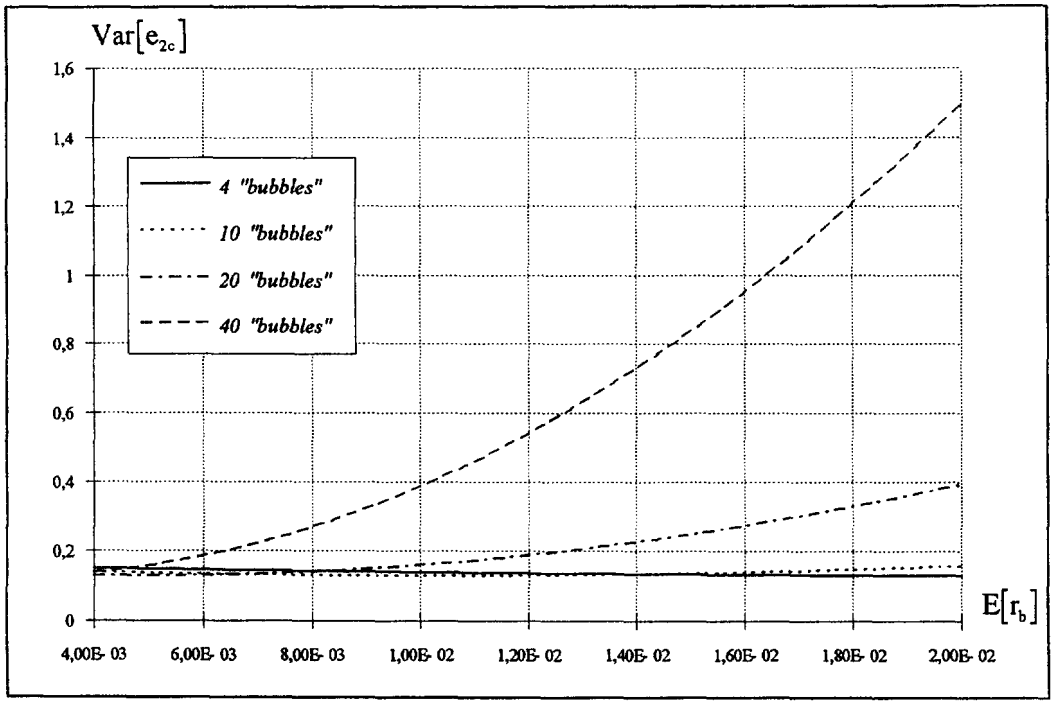

Fig. 15. Variances of homogenized Young's modulus in matrix region.

location of the point on the fiber–matrix boundary with respect to the x or y-coordinate on the tensioned face is marked on the vertical axes.

The first observation is the significant influence of the matrix discontinuities on the stochastic displacement fields and the negligible changes of these displacements with respect to the fiber defects (cf. Table 1). Primarily this is caused by an assumed small coefficient of variation for the Young's modulus in the fiber in relation to the matrix and the interrelation of the geometric approximation of these defects on both sides of the interface. Moreover, this influence is highly sensitive to the relation between the coefficients of variation of the elastic constants and the contact zone geometry in the composite phases.

A further general observation is the direct proportionality between the number of interface defects and the volume of the contact zone, and the expected values or the coefficients of variation of these displacements. Small differences occur in case of the interface expected values of displacements for larger β angles.

By comparing the coefficients of variation of interface displacements (Figs 16 and 17) we observe quite different forms for the relation between these coefficients and the β angle: the model with a large contact zone shows a high sensitivity to the number of defects. Changes for the small contact zone are proportional. In the case of the coefficients of the

Table 1. Expected values of interface displacements for different number of fiber defects

	Small contact zone			Large contact zone		
β [°]	0% "teeth"	25% "teeth"	50% "teeth"	0% "teeth"	25% "teeth"	50% "teeth"
0	5.005×10^{-4}	5.012×10^{-4}	5.007×10^{-4}	4.970×10^{-4}	4.970×10^{-4}	4.969×10^{-4}
11.25	4.970×10^{-4}	4.968×10^{-4}	4.972×10^{-4}	4.961×10^{-4}	4.962×10^{-4}	4.962×10^{-4}
22.5	5.137×10^{-4}	5.138×10^{-4}	5.140×10^{-4}	4.938×10^{-4}	4.938×10^{-4}	4.939×10^{-4}
33.75	5.952×10^{-4}	5.960×10^{-4}	5.960×10^{-4}	4.901×10^{-4}	4.900×10^{-4}	4.900×10^{-4}
45	7.182×10^{-4}	7.182×10^{-4}	7.184×10^{-4}	4.850×10^{-4}	4.851×10^{-4}	4.851×10^{-4}
56.25	8.279×10^{-4}	8.285×10^{-4}	8.289×10^{-4}	4.865×10^{-4}	4.864×10^{-4}	4.865×10^{-4}
67.5	9.397×10^{-4}	9.400×10^{-4}	9.404×10^{-4}	4.893×10^{-4}	4.893×10^{-4}	4.893×10^{-4}
78.75	12.876×10^{-4}	12.881×10^{-4}	12.885×10^{-4}	4.978×10^{-4}	4.972×10^{-4}	4.966×10^{-4}
90	37.052×10^{-4}	37.565×10^{-4}	38.082×10^{-4}	24.786×10^{-4}	24.095×10^{-4}	23.390×10^{-4}

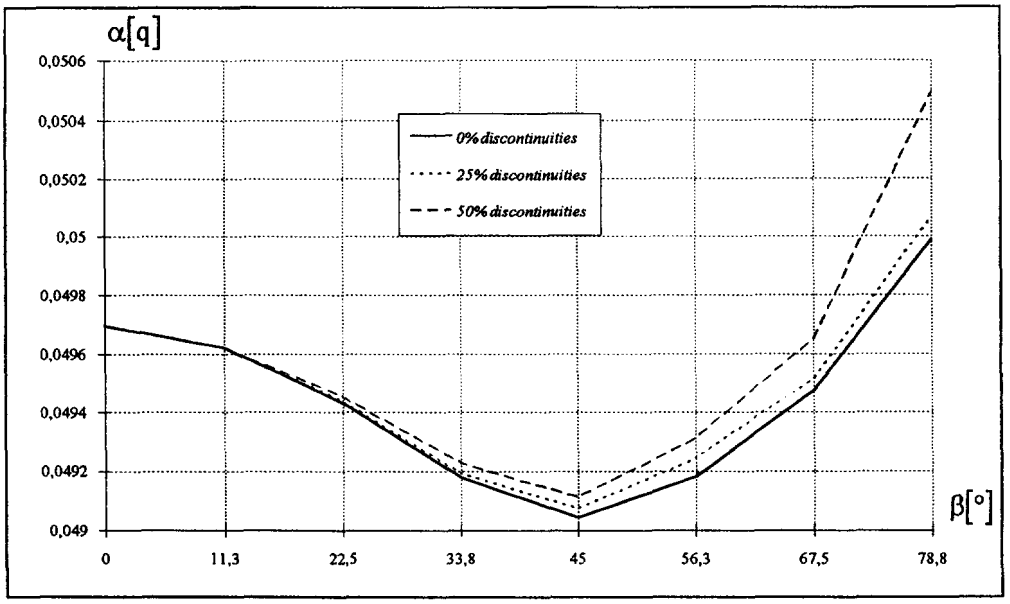

Fig. 16. Coefficients of variation of interface displacements for small contact zone.

tensioned edge horizontal displacement variation both the models give approximately reversed effects (Figs 20 and 21). For example a small contact zone causes larger coefficients for smaller β values than for larger β (Fig. 20). On both sizes of the contact zones the changes in the α coefficient are inversely proportional to the increase in number of discontinuities and consequently the relations given in Figs 17 and 21 show some similarity.

Finally, in both the models the expected values of displacement are quite similar with respect to their locations. In the large contact zone (Figs 19 and 23) the differences between obtained expected values of displacements for 0%, 25% and 50% of discontinuities are more significant.

4. CONCLUSIONS AND RECOMMENDATIONS

(1) The approach presented here for solving the contact problem appears to allow for the first time a direct consideration of the random character of the contact zone geometry,

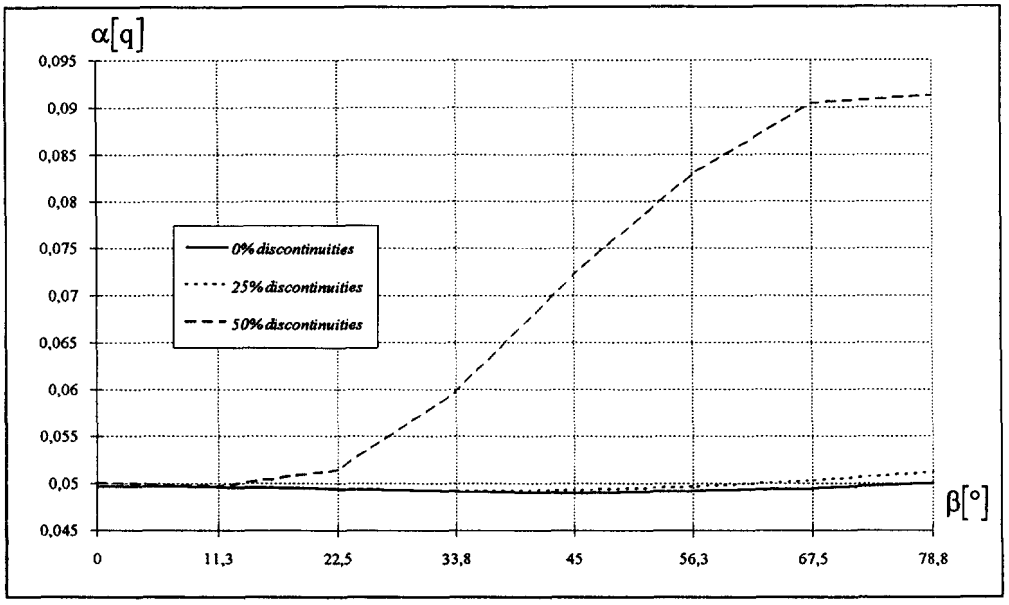

Fig. 17. Coefficients of variation of interface displacements for large contact zone.

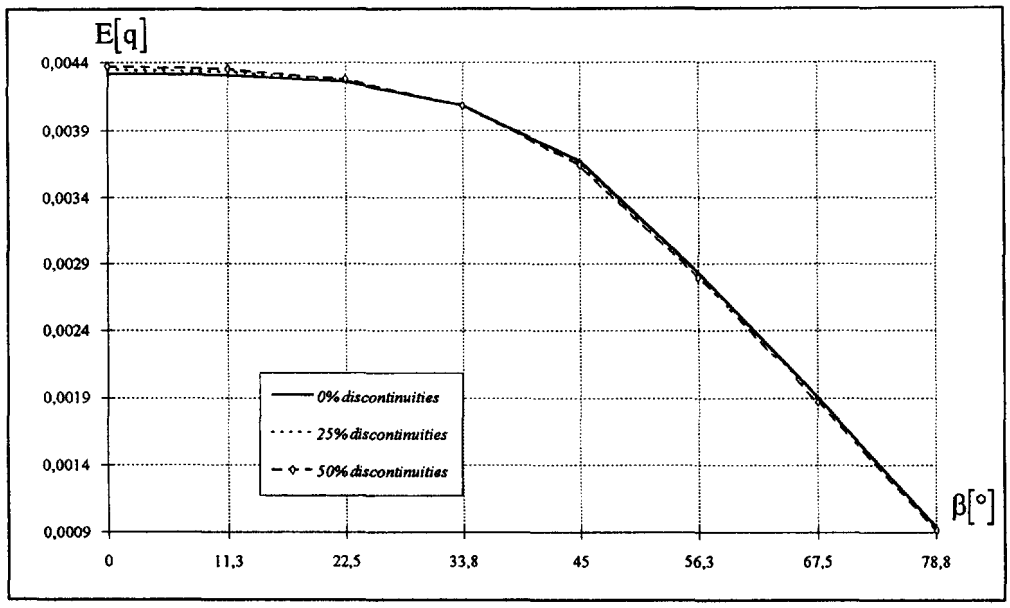

Fig. 18. Expected values of interface displacements for small contact zone.

at the same time including the randomness of elastic behavior of composite components. Numerical results obtained by this method show that the interface defects located in the matrix contact zone have a major influence on the stochastic displacement fields of a quarter model of the composite periodicity cell. This result, however, strongly depends on interrelation of variation in Young's modulus in both composite phases and the approximation of the contact zones geometry.

(2) Homogenization, as used in this paper, is only an intermediate tool used to obtain an equivalent material with a stochastic character in the contact zone defined in a deterministic way. Since this averaging is done in a region of relatively small size in comparison with the overall dimensions of the whole structure, errors resulting from such simplification should be less than those resulting from the assumed approach to the contact problem. However, it would be interesting to formulate, similarly to the deterministic

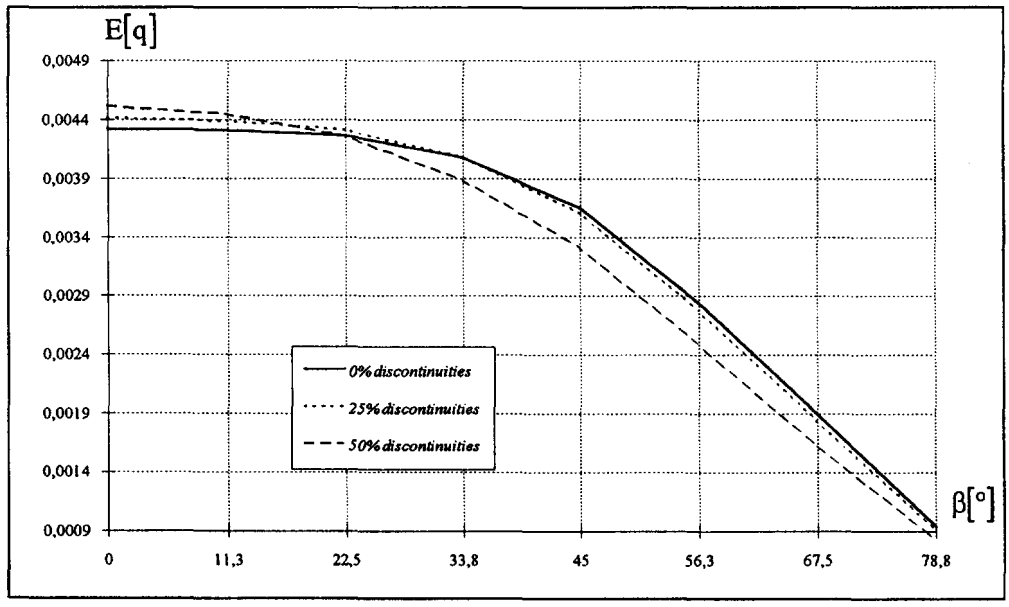

Fig. 19. Expected values of interface displacements for large contact zone.

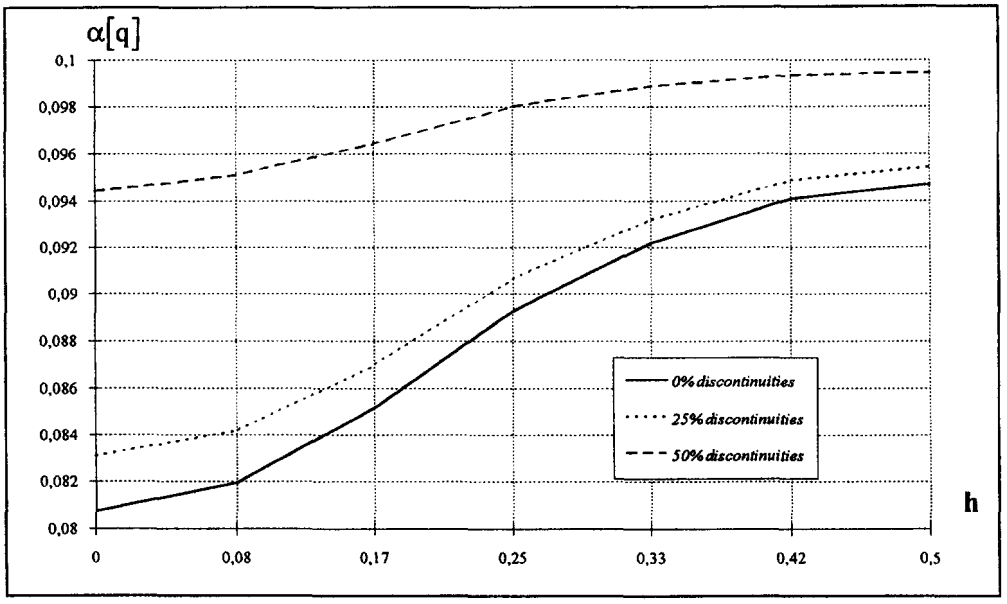

Fig. 20. Coefficients of variation of tensioned edge horizontal displacements for small contact zone.

models (Bensoussan *et al.*, 1978; Lené, 1984; Telega, 1988), the stochastic composite homogenization problem with random interface defects.

(3) A further novelty in the development of this technique for contact problems would be the construction of an appropriate plane stochastic finite element. Such an element, for given parameters of discontinuities distribution, would homogenize properties of the material within its region. It would enable the analysis of the influence of discontinuity localization around the fiber circumference on a random displacement state as well as stresses in a periodicity cell. Due to the mathematical–numerical formulation presented here it is possible to average these discontinuities only uniformly along the whole fiber circumference. Moreover, it would be possible to implement the different shapes of defects (triangles, rectangles or hexagonals for example).

(4) Finally, there remains the interesting problem of sensitivity of a periodic fiber

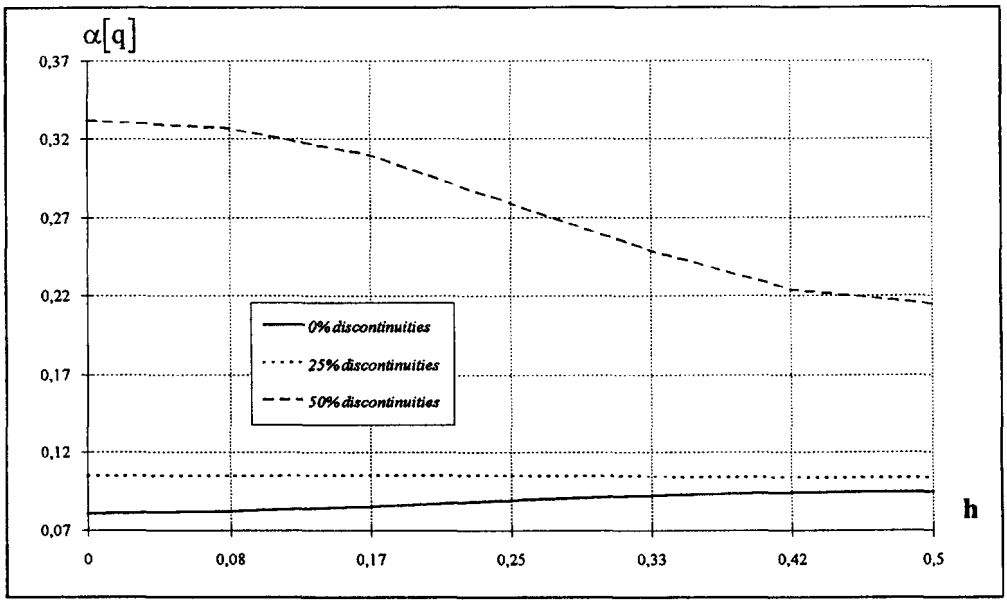

Fig. 21. Coefficients of variation of tensioned edge horizontal displacements for large contact zone.

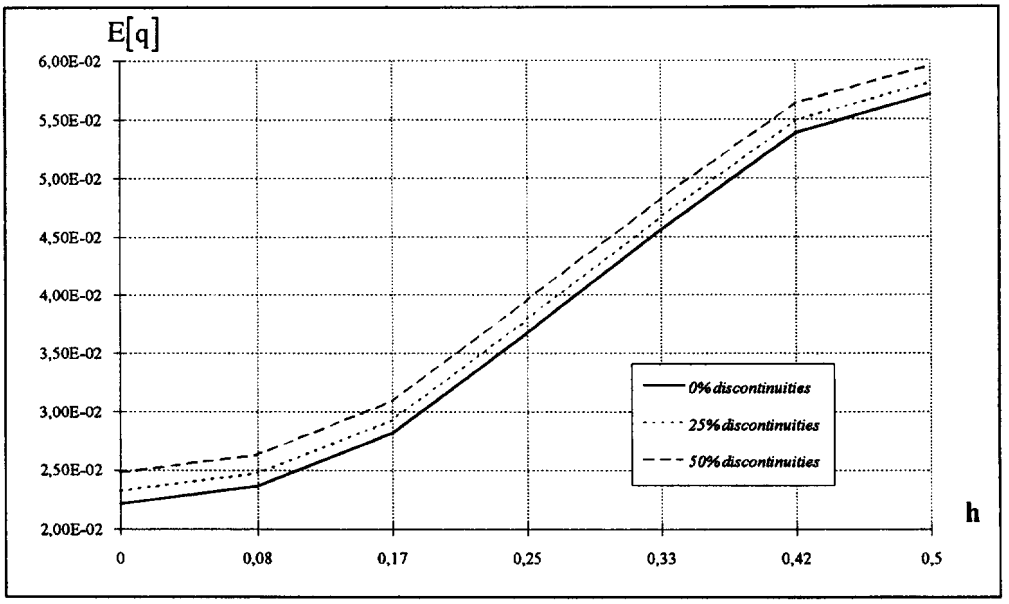

Fig. 22. Expected values of tensioned edge horizontal displacements for small contact zone.

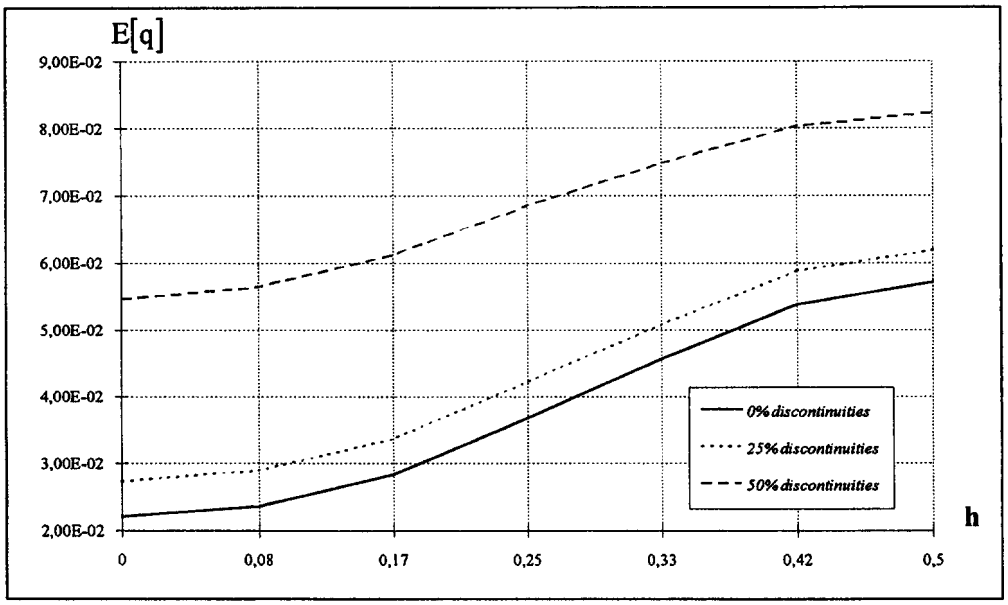

Fig. 23. Expected values of tensioned edge horizontal displacements for large contact zone.

composite with random interface defects. This can be formulated as stochastic sensitivity of the displacement fields with respect to the random shape of matrix contact zone boundary (Dems and Haftka, 1988–1989; Dems and Mróz, 1987). This problem seems to be important when considering the main influence of the contact zone and the stochastic character of the matrix material on expected values and covariances of the displacements. It would be possible to solve this problem with the particular kind of stochastic interface element discussed above.

Acknowledgements—This paper was supported by the Polish State Committee for the Scientific Research, project no. 8 T11F 010 09.

REFERENCES

Aboudi, J. (1991). *Mechanics of Composite Materials—a Unified Micromechanical Approach*. Elsevier, Amsterdam.

Achenbach, J. D. and Choi, H. S. (1991). Matrix cracking and interphase failure in fiber composites. In *Local Mechanics Concepts for Composite Material Systems* (Edited by J. N. Reddy and K. L. Reifsnider), pp. 149–163. IUTAM Symposium Blacksburgh, Springer, Berlin.

Adams, D. F. (1970). Inelastic analysis of a unidirectional composite subjected to transverse normal loading. *J. Compos. Mater.* **4,** 310–328.

Arminjon, M. (1991). Limit distributions of the states and homogenization in random media. *Acta Mech.* **88,** 27–59.

Ashton, J. E., Halpin, J. C. and Petit, P. H. (1969). *Primer on Composite Materials: Analysis*. Connecticut.

Avellaneda, M. (1987). Optimal bounds and microgeometries for elastic two-phase composites. *SIAM J. Appl. Math.* **47,** 1216–1228.

Bahei-El-Din, Y. A., Dvorak, G. J. and Utku, S. (1981). Finite element analysis elasto-plastic fibrous composite structures. *Comput. Struct.* **13,** 321–330.

Barry, P. W. (1978). The longitudinal tensile strength of unidirectional fibrous composites. *J. Mater. Sci.* **13,** 2177–2187.

Batdorf, S. B. (1978). Fundamentals of the statistical theory of fracture. In *Fracture Mechanics of Ceramics* (Edited by R. C. Bradt, D. P. H. Hasselman and F. M. Lange), pp. 1–30. Plenum, New York.

Batdorf, S. B. and Ghaffarian, R. (1984). Size effect and strength variability of unidirectional composites. *Int. J. Fracture* **26,** 113–123.

Bathe, K. J., Wilson, E. L. and Peterson, F. E. (1973). *SAP IV—A Structural Analysis Program for Static and Dynamic Response of Linear Systems. Technical Report*. College of Engineering, University of California.

Bensoussan, A., Lions, J. L. and Papanicolau, G. (1978). *Asymptotic Analysis for Periodic Structures*. North-Holland, Amsterdam.

Benveniste, Y. (1985). The effective mechanical behavior of composite materials with imperfect contact between the constituents. *Mech. Mater.* **4,** 197–208.

Benveniste, Y., Chen, T. and Dvorak, G. J. (1990). The effective thermal conductivity of composites reinforced by coated cylindrically orthotropic fibers. *J. Appl. Phys.* **67,** 2878–2884.

Beran, M. J. (1968). Statistical continuum theories. In *Monographs in Statistical Physics and Thermodynamics*. Wiley, New York.

Budiansky, B. (1965). On the elastic moduli of some heterogeneous materials. *J. Mech. Phys. Sol.* **13,** 223–227.

Caruso, J. J. and Chamis, C. C. (1986). Assessment of simplified composite micromechanics using three-dimensional finite element analysis. *J. Compos. Tech. Res.* **8,** 77–83.

Chang, S., Chao, S. J. and Chang, Y. (1995). Estimates of elastic moduli for granular material with anisotropic random packing structure. *Int. J. Solids Struct.* **32,** 1989–2008.

Chen, H. S. and Acrivos, A. (1978). The effective elastic moduli of composite materials containing spherical inclusions at non-dilute concentrations. *Int. J. Solids Struct.* **14,** 349–364.

Choi, H. S. and Achenbach, J. D. (1995). Stress states at neighboring fibers induced by single-fiber interphase defects. *Int. J. Solids Struct.* **32,** 1555–1570.

Christensen, R. M. (1979). *Mechanics Composite Materials*. Wiley-Interscience, New York.

Dems, K. and Haftka, R. T. (1988–89). Two approaches to sensitivity analysis for shape variation of structures. *Mech. Struct. Mach.* **16,** 501–522.

Dems, K. and Mróz, Z. (1987). Variational approach to sensitivity analysis in thermoelasticity. *J. Therm. Struct.* **10,** 283–306.

Drucker, D. C. (1975). Yielding, flow and fracture. In *Inelastic Behaviour of Composite Materials* (Edited by C. T. Herakovich), pp. 1–15. ASME, New York.

Dvorak, G. J. and Rao, M. S. M. (1976). Axisymmetric plasticity theory of fibrous composites. *Int. J. Engng Sci.* **14,** 361–373.

Fisher, R. A. (1971). *The Design of Experiments*. Hafner Press, New York.

Gajl, O. (1990). Effective properties of cracked composites. *Proc. Int. Polish-German Symposium*, Bad-Honnef.

Hashin, Z. (1965). On elastic behaviour of fiber reinforced materials of arbitrary transverse phase geometry. *J. Mech. Phys. Solid.* **13,** 119–134.

Hashin, Z. (1972). *Theory of Fiber Reinforced Materials*. NASA, Hampton, VA.

Hashin, Z. (1990). Thermoelastic properties of fiber composites with imperfect interface. *Mech. Mater.* **8,** 333–348.

Hashin, Z. and Shtrikman, S. (1963). A variational approach to the theory of elastic behaviour of multiphase materials. *J. Mech. Phys. Solids* **11,** 127–140.

Haug, E. J., Choi, K. K. and Komkov, V. (1986). *Design Sensitivity Analysis of Structural Systems*. Academic Press, New York.

Hien, T. D. (1990). *Deterministic and Stochastic Sensitivity in Computational Structural Mechanics*. Habilitation Thesis, IFTR PAS 46(90), Warsaw.

Hill, R. (1964). Theory of mechanical properties of fiber-strengthened materials I. Elastic behaviour. *J. Mech. Phys. Solids* **12,** 199–212.

Jasiuk, I., Chen, J. and Thorpe, M. F. (1992). Elastic moduli of composites with rigid sliding inclusions. *J. Mech. Phys. Solids* **40,** 373–391.

Kamiński, M. (1996). Homogenization in elastic heterogeneous random media. *Comput. Ass. Mech. Engng Sci.*, in press.

Kamiński, M. (1995). Stochastic contact effects in periodic fiber composites. *J. Theor. Appl. Mech.* **33,** 415–441.

Kamiński, M. and Gajl, O. (1995). Numerical modelling of fiber composites with random-elastic components. *Comput. Ass. Mech. Engng Sci.* **2,** 41–50.

Kelly, A. (1989). *Concise Encyclopedia of Composite Materials*. Pergamon Press, Oxford.

Kleiber, M. and Hien, T. D. (1992). *The Stochastic Finite Element Method. Basic Perturbation Technique and Computer Implementation*. Wiley, New York.

Lené, F. (1984). Contribution a l'etude des materiaux composites et de leur endommagement. These du Doctorat d'Etat, Universite Paris VI, Paris.

Liu, W. K., Belytschko, T. and Mani, A. (1986). Random field finite elements. *Int. J. Numer. Meth. Engng* **23,** 1831–1845.

Milton, G. W. and Kohn, R. V. (1988). Variational bounds on the effective moduli for anisotropic composites. *J. Mech. Phys. Solids* **36,** 597–630.

Mital, S. K., Murthy, P. L. N. and Chamis, C. C. (1993). Interfacial microstructure in high temperature metal matrix composites. *Int. J. Compos. Mater.* **27,** 1678–1694.

Moavenzadeh, F. (1990). *Concise Encyclopedia of Building & Construction Materials.* Pergamon Press, Oxford.

Mori, T. and Tanaka, K. (1973). Average stress in matrix and average elastic energy of materials with misfitting inclusions. *Acta Metall.* **21,** 571–574.

Murthy, P. L. N. and Chamis, C. C. (1992). Towards the development of micromechanics equations for ceramic matrix composites via fiber substructuring. NASA TM-105246.

Noor, A. K. and Shah, R. S. (1993). Effective thermoelastic and thermal properties of unidirectional fiber-reinforced composites and their sensitivity coefficients. *Comput. Struct.* **26,** 7–23.

Ostoja-Starzewski, M. and Wang, C. (1989). Linear elasticity of planar Delaunay networks: random field characterization of effective moduli. *Acta Mech.* **80,** 61–80.

Phoenix, S. L. and Smith, R. L. (1983). A comparison of probabilistic techniques for the strength of fibrous materials under local load sharing. *Int. J. Solids Struct.* **19,** 479–496.

Phoenix, S. L. and Tierney, L. J. (1983). A statistical model for the time dependent failure of unidirectional composite materials under local elastic load sharing among fibers. *Engng Fracture Mech.* **18,** 193–215.

Sab, K. (1992). On the homogenization and the simulation of random materials. *Eur. J. Mech. Solids* **11,** 585–607.

Sendeckyj, G. P. (1974). *Composite Materials*, Vol. 2, *Mechanics of Composite Materials.* Academic Press, New York.

Sobczyk, K. (1982). *Stochastic Wave Propagation.* PSB, Warsaw.

Suquet, P. (1982). Plasticite et homogeneisation. These de Doctorat d'Etat, Universite Paris VI, Paris.

Telega, J. J. (1988). Variational inequalities in mechanical contact problems. In *Contact Surface Mechanics* (Edited by Z. Mróz), pp. 56–165. IFTR PAS.

Tsai, S. W. and Wu, E. M. (1971). A general theory of strength for anisotropic materials. *Int. J. Compos. Mater.* **5,** 58–80.

Wriggers, P. and Zavarise, G. (1993). Application of augmented lagrangian techniques for nonlinear constitutive laws in contact interfaces. *Commun. Numer. Meth. Engng* **9,** 815–824.

Zavarise, G., Wriggers, P., Stein, E. and Schrefler, B. A. (1992a). A numerical model for thermomechanical contact based on microscopic interface laws, *Mech. Res. Comm.* **19,** 173–182.

Zavarise, G., Wriggers, P., Stein, E. and Schrefler, B. A. (1992b). Real contact mechanisms and finite element formulation—a coupled thermomechanical approach. *Int. J. Num. Meth. Engng* **35,** 767–785.

Zweben, C. and Rosen, B. W. (1970). A statistical theory of material strength with application to composite materials. *J. Mech. Phys. Solids* **18,** 189–206.